

Characterization of F-Actin Tryptophan Phosphorescence in the Presence and Absence of Tryptophan-Free Myosin Motor Domain

Emőke Bódis,* Giovanni B. Strambini,[†] Margherita Gonnelli,[†] András Málnási-Csizmadia,[‡] and Béla Somogyi*

*Hungarian Academy of Sciences, Research Group for Fluorescence Spectroscopy, Office for Academy Research Groups Attached to Universities and Other Institutions, 7624 Pécs, Hungary; [†]Consiglio Nazionale delle Ricerche, Istituto di Biofisica, 56100 Pisa, Italy; and [‡]Eötvös Loránd University, Department of Biochemistry, 1117 Budapest, Hungary

ABSTRACT The effect of binding the Trp-free motor domain mutant of *Dictyostelium discoideum*, rabbit skeletal muscle myosin S1, and tropomyosin on the dynamics and conformation of actin filaments was characterized by an analysis of steady-state tryptophan phosphorescence spectra and phosphorescence decay kinetics over a temperature range of 140–293 K. The binding of the Trp-free motor domain mutant of *D. discoideum* to actin caused red shifts in the phosphorescence spectrum of two internal Trp residues of actin and affected the intrinsic lifetime of each emitter, decreasing by roughly twofold the short phosphorescence lifetime components (τ_1 and τ_2) and increasing by ~20% the longest component (τ_3). The alteration of actin phosphorescence by the motor protein suggests that i), structural changes occur deep down in the core of actin and that ii), subtle changes in conformation appear also on the surface but in regions distant from the motor domain binding site. When actin formed complexes with skeletal S1, an extra phosphorescence lifetime component appeared (τ_4 , twice as long as τ_3) in the phosphorescence decay that is absent in the isolated proteins. The lack of this extra component in the analogous actin-Trp-free motor domain mutant of *D. discoideum* complex suggests that it should be assigned to Trps in S1 that in the complex attain a more compact local structure. Our data indicated that the binding of tropomyosin to actin filaments had no effect on the structure or flexibility of actin observable by this technique.

INTRODUCTION

In the course of the contraction cycle of the actomyosin system, the large structural changes of myosin are widely studied, whereas the structural changes of actin are less investigated. It is known that actin conformation changes dramatically during its polymerization; however, much less structural changes can be detected when it binds to myosin.

Spectroscopic methods proved to be powerful experimental tools to study the conformation and dynamics of different proteins (Somogyi et al., 2000; Nyitrai et al., 1998,1999; Somogyi and Lakos, 1993; Silva and Prendergast, 1996; Lorinczy et al., 2002; Berger and Thomas, 1993; Ostap and Thomas, 1991; Zavodszky et al., 1998; Lakos et al., 1990). Applying phosphorescence spectroscopy, we aimed to investigate the structural changes of actin during its complex formation with myosin for a better understanding of the significance of actin in the ATPase turnover and force generation. Actin contains four Trp residues as intrinsic fluorophores; all of them are located in subdomain I (Fig. 1),

which on its surface bears most of the amino acids that bind to myosin (Fig. 2). Due to the proximity of the aromatic probes to the actin-myosin interactive surface, their intrinsic luminescence may be a sensitive tool to the potential changes, which may occur on formation of the actin-myosin complex. Producing the Trp-free *Dictyostelium discoideum* motor domain construction (Malnasi-Csizmadia et al., 2000), the effect of myosin on the Trp fluorescence of actin was investigated. According to the results, a small but significant change of the Trp fluorescence was observed (Wakelin et al., 2002). The phosphorescence of the Trps of actin can provide a more sensitive multisite probe of protein structure and dynamics (Vanderkooi, 1992; Schauerte et al., 1997). The spectral energy of phosphorescence emission reports on the polarity of their immediate environment (Hershberger et al., 1980), whereas the excited state lifetime is a sensitive monitor of the local fluidity of the protein matrix (Gonnelli and Strambini, 1995). The latter parameter has shown to exhibit a remarkable sensitivity for uncovering subtle changes in conformation in several enzymes that are brought about by the binding of substrates and allosteric effectors (Cioni and Strambini, 1989; Gabellieri et al., 1996; Strambini and Gonnelli, 1990), changes otherwise undetected with conventional spectroscopic techniques. As part of a more general enquiry on the structure of actin filaments, this study explores possible changes in the conformation of actin that may be induced by the formation of binary and ternary complexes with a Trp-free *D. discoideum* motor domain or rabbit skeletal myosin S1 and the naturally Trp-free tropomyosin.

Submitted February 23, 2004, and accepted for publication April 27, 2004.

Address reprint requests to Prof. Béla Somogyi, Dept. of Biophysics, University of Pécs, Faculty of Medicine, Szigeti str. 12, H-7624 Pécs, Hungary. Tel.: 36-72-536260; Fax: 36-72-536261; E-mail: somogyi.publish@aok.pte.hu.

Abbreviations used: MD/W–, Trp-free motor domain mutant of *Dictyostelium discoideum*; S1, myosin subfragment 1; Tm, tropomyosin; Tes, *N*-Tris(hydroxymethyl)methyl-2-aminoethanesulfonic acid; PMSF, phenylmethylsulfonyl fluoride; MEA, 2-mercaptoethanol; DTT, dithiothreitol; TEMED, *N,N,N',N'*-tetramethylethylenediamine; SDS, sodium dodecyl sulfate; PEP, phosphoenolpyruvate.

© 2004 by the Biophysical Society

0006-3495/04/08/1146/09 \$2.00

doi: 10.1529/biophysj.104.041855

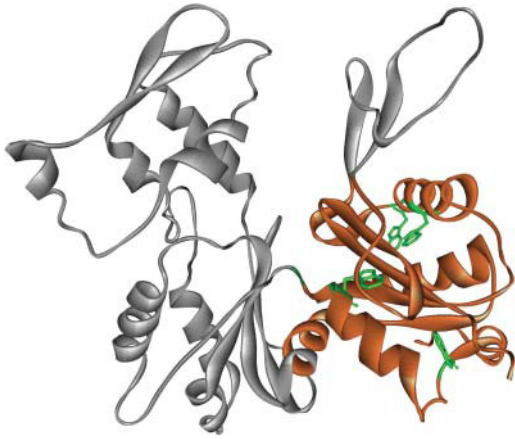


FIGURE 1 Solid ribbon model of actin monomer according to x-ray data from the Protein Data Bank, code 1ATN. The subdomain I is colored orange and the Trps are marked.

A preliminary investigation of the phosphorescence emission of G- and F-actin has shown that both the spectrum and the decay kinetics of its four Trp residues are markedly heterogeneous, suggesting that their environment varies considerably in both polarity and local flexibility (Strambini and Lehrer, 1991). Since this initial report, considerable improvements have been achieved in both spectral and lifetime resolution, the latest instrumentation permitting to characterize the entire range of Trp emission in proteins (Strambini and Gonnelli, 1995; Gonnelli and Strambini, 1995). In this work, we take advantage of the new potentialities of the technique to reexamine the phosphorescence characteristics of F-actin and use these probes to monitor possible changes in the conformation of the globular structure that may be associated with the complex formation with Tm and S1. In the case of S1, to avoid interference from the emission of Trp residues in the motor protein, parallel experiments were carried out with the Trp-free *D. discoideum* motor domain. The results describe an almost complete characterization of the phosphorescence emission of each Trp residue of F-actin. They point out that changes in conformation do occur in subdomain I but only upon complexation to

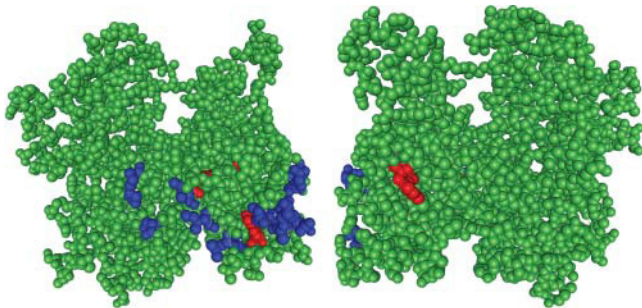


FIGURE 2 Corey-Pauling-Koltun (CPK) model of actin monomer from the front and back position. The myosin binding sites are colored dark blue, and the Trps of actin are colored red.

MD/W- or to S1. On the other hand, the lack of any structuring effect of Tm binding, in either binary or ternary complexes with the motor protein, is fully consistent with the three-state dynamic steric model of thin filament regulation (McKillop and Geeves, 1993).

MATERIALS AND METHODS

Reagents

Tes, Tris, Na_2HPO_4 , MgCl_2 , CaCl_2 , NaCl, KCl, NaOH, α -chymotrypsin, PMSF, EDTA, EGTA, MEA, DTT, NaN_3 , and $(\text{NH}_4)_2\text{SO}_4$ were obtained from Sigma Chemical (St. Louis, MO). ATP, glycerol was obtained from Merck (Darmstadt, Germany), TEMED, Coomassie protein micro-assay from Bio-Rad (Hercules, CA), and SDS is from United States Biochemical (Cleveland, OH). Water, doubly distilled over quartz, was purified by using a Milli-Q Plus system (Millipore, Bedford, MA). All glassware used for sample preparation was conditioned in advance by standing for 24 h in 10% HCl suprapur (Merck). All chemicals were of the highest purity grade available from commercial sources and used without further purification.

Protein preparation

Actin (Spudich and Watt, 1971), myosin (Margossian and Lowey, 1982), and tropomyosin (Smillie, 1982) were prepared from rabbit skeletal muscle. S1 was prepared by α -chymotrypic digestion of myosin (Weeds and Taylor, 1975). *D. discoideum* motor domain Trp-free mutant was cloned and prepared as described in Malnasi-Csizmadia et al. (2000). Concentrations of G-actin (Houk and Ue, 1974), S1 (Wagner, 1977), and tropomyosin (Smillie, 1982) were determined from absorption data using the extinction coefficient of $\epsilon_{290\text{nm}}^{1\%} = 6.3$, $\epsilon_{280\text{nm}}^{1\%} = 7.5$, and $\epsilon_{280\text{nm}}^{1\%} = 2.4$, respectively.

Phosphorescence measurements

Before phosphorescence measurements, actin was dialysed against 2 mM Tris, pH 8.0, 0.2 mM ATP, and 0.1 mM CaCl_2 . G-actin was polymerised by adding 100 mM KCl and 2 mM MgCl_2 to the solution. MD/W-, S1, and Tm were dialysed against 2 mM Tris, pH 8.0, 100 mM KCl, and 2 mM MgCl_2 . In all samples, the final concentration of the actin was maintained between 10 and 15 μM . For low temperature studies, the samples contained 60% glycerol. For phosphorescence measurements at ambient temperature, it is paramount to rid the solution of all O_2 traces. Protein samples were placed in appositely constructed quartz cuvettes (round 4-mm cells for low temperature studies in glasses and square, $5 \times 5 \text{ mm}^2$, cells for measurements in buffer above freezing temperature) and were deoxygenated by repeated cycles of mild evacuation followed by the inlet of pure nitrogen as described before (Gonnelli and Strambini, 1995).

The biological functioning of S1 were routinely characterized by measuring the K^+/EDTA -, Ca^{2+} -ATPase activity by the determination of phosphate release (Fiske and Subbarow, 1925). The assays were performed at room temperature in 50 mM Tris-HCl, pH 8.0, 0.6 M KCl, and 2.5 mM ATP and either 10 mM EDTA or 9 mM CaCl_2 . To characterize the biological activity of MD/W-, the Mg^{2+} -ATPase activity was measured by using the coupled enzyme assay (Norby, 1971). These experiments were carried out in 20 mM Mops, pH 7.0, 100 mM KCl, 1 mM MgCl_2 , 0.5 mM ATP, 1 mM PEP, 0.5 mM EGTA, 0.15 mM NADH, 200 units/ml pyruvate kinase, and 400 units/ml lactate dehydrogenase. The conversion of NADH to NAD^+ (molar equivalent to the hydrolysis of ATP) was monitored by measuring the absorbance at 340 nm. The activity of these proteins was not affected by keeping them in 60% glycerol (a protein stabilizing cosolvent) and taking them to low temperature during the phosphorescence measurements.

All luminescence measurements were conducted on homemade instrumentation. For emission spectra, continuous excitation is provided by a Cemax xenon lamp (LX150UV, ILC Technology, Sunnyvale, CA) whose output is a selected (6-nm bandpass) emission wavelength of 295 nm by a 0.23-m double grating monochromator (SPEX, model 1680, Spex Industries, Edison, NJ) optimized for maximal stray light rejection. The emission collected at 90° from the excitation is dispersed by a 0.25-m grating monochromator (Jobin-Yvon, H-25, Lille, France) set to a bandpass of 0.2 nm. A two positions light chopper intersects either the excitation beam only (fluorescence mode) or both excitation and emission beams in an alternate fashion in such a way that only delayed emission gets through to the detector (phosphorescence mode). A low-noise current preamplifier (Stanford Research Systems, model SR570, Sunnyvale, CA) followed by a lock-in amplifier (ITHACO, model 393, Ithaca, NJ) operated at the chopper frequency are used to amplify the photomultiplier (EMI 9635QB, Rockaway, NJ) current. The output is digitized and stored by a multifunction board (PCI-20428W, Intelligent Instrumentation, Tucson, AZ) utilizing visual Designer software (PCI-20901S ver. 3.0, Intelligent Instrumentation). Spectra are acquired at a scan rate of 0.1 nm s⁻¹ and with a time constant (lock-in amplifier) of 125 ms. Phosphorescence spectra were obtained at an excitation wavelength of 295 nm where Tyr absorption is relatively small. Trp spectra were corrected for the weak emission of Tyr, any ADP/ATP, and the solvent background by using as a blank the spectrum of Tm, which contains Tyr but not Trps, in the same solvent. Before subtraction, the control spectrum was normalized to have the same intensity below 390 nm, a region free of Trp phosphorescence.

For phosphorescence decays, pulsed excitation is provided by a frequency-doubled, Nd/Yag-pumped dye laser (Quanta Systems, Milan, Italy; $\lambda_{ex} = 292$ nm) with a pulse duration of 5 ns and a typical energy per pulse of 0.5–1 mJ. The phosphorescence emitted at 90° from the excitation is selected by an interference filter (DTblau, Balzer, Milan, Italy) with a transmission window between 410 and 450 nm. The photomultiplier (EMI 9235QA) is protected from the intense fluorescence pulse by a chopper blade that closes the emission slit during the excitation. The time resolution of this apparatus is typically 10 μ s (Strambini and Gonnelli, 1995). The photocurrent is amplified by a low noise current to voltage converter (SR570, Stanford Research Systems) and digitized by a computer scope system (ISC-16, RC Electronics, Santa Barbara, CA) capable of averaging multiple sweeps. All phosphorescence decays were analyzed in terms of a sum of exponential components by a nonlinear least-square fitting algorithm (Global Unlimited, LFD, University of Illinois, Urbana-Champaign, IL). In all cases, three exponential components gave a remarkably better fit than two exponential components. All reported lifetimes are averages of two or more independent measurements, and the reproducibility of lifetime determinations was typically better than 5%.

X-ray structure

The x-ray model of actin monomer was downloaded from the Protein Data Bank, code 1ATN. The structure of the molecule can be visualized by RasMol software (<http://www.rasmol.org/>). The B-factor, calculated by software, represents the mean-square displacement of an atom about its central position and is taken as an indicator of its thermal mobility in a molecule. Large B-factors may also be associated to a structural disorder arising from heterogeneous protein conformations in the crystal.

RESULTS

Trp phosphorescence of F-actin

In glasses at low temperature, the phosphorescence spectrum of Trp exhibits a pronounced vibronic structure with a relatively narrow 0,0 vibrational band. The wavelength of the 0,0 band ($\lambda_{0,0}$) is related to the polarity of the indole

environment (Hershberger et al., 1980), and its bandwidth reports on the structural homogeneity of the site. Often, depending on the strength of the interaction with the protein matrix, two or more Trp residues in the same polypeptide may exhibit well resolved 0,0 vibrational bands, and their emission can be studied individually. The spectrum of F-actin, in a glycerol/buffer glass at 140 K, exhibits two relatively broad but energetically distinct 0,0 vibrational bands centered at 404.5 and 415.6 nm (Fig. 3 A); the large energy separation between them indicates two classes of chromophores making strong but opposite dipolar interactions with their surrounding. The high energy spectral component (404.5 nm) is blue shifted with respect to the spectrum of free Trp in the same solvent (406.4 nm) and should probably be assigned to residues that are on the surface and partly exposed to the polar solvent. Support for this assignment comes from the thermal quenching/spectral relaxation profile as this band shifts to the red and decreases in intensity relatively early during the warming up of the sample (Strambini and Lehrer, 1991), roughly in the same temperature range as fully exposed Trp residues. The red band is broad and composite, with peaks at 414.1 and 416.7 nm. It originates from buried residues whose triplet state energy is lowered, relative to a nonpolar site (411–412 nm), by favorable interactions with some local dipole or charged side chain. The distinction into two components of the red band was not evident in the previous lower resolution study of actin phosphorescence (Strambini and Lehrer, 1991).

Above 190 K, the glass softens into a fluid solution and the polypeptide recovers its natural flexibility. As a result, both the phosphorescence lifetime and quantum yield decrease steeply due to the enhancement of nonradiative transitions in fluid media. Thermally activated intramolecular quenching reactions may also contribute to the lifetime shortening (Gonnelli and Strambini, 1995). In accord with the previous report (Strambini and Lehrer, 1991), the spectrum and lifetime thermal profile of F-actin (not shown) confirm that the blue band is selectively quenched between 190 and 230 K and that the red emitting Trps are responsible for the long-lived emission in fluid solutions. As mentioned above, the transition temperature of the blue band is typical of free Trp in solvent and strengthens the assignment of the blue band to superficial or solvent exposed residues. Above 230 K, the red band sharpens around a maximum at 417 nm and, apart from becoming slightly broader, remains unaltered up to the ambient temperature. The narrowing of the red band can result from either the relaxation of the 414.1-nm component to higher wavelengths or from its decrease in quantum yield after a temperature induced decrease in lifetime.

The great variability in phosphorescence lifetime among the Trp residues of actin manifested in the multiphase thermal quenching profile in glycerol/buffer is also observed in the highly heterogeneous phosphorescence decay in buffer. Fig. 4 shows the Trp phosphorescence decay of actin at 0.5°C, and Table 1 collects the lifetime values derived

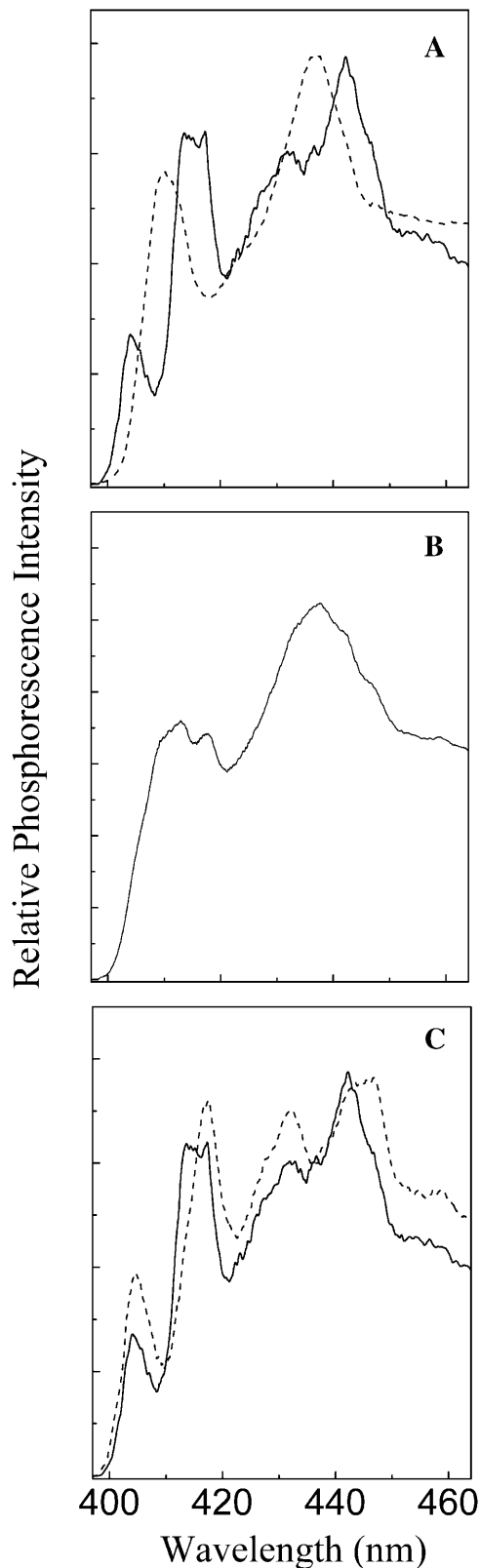


FIGURE 3 Trp phosphorescence spectrum of F-actin, S1, and their binary complex in a glycerol/buffer (60:40, w/w) glass at 140 K. (A) Comparison between F-actin (solid line) and S1 (dashed line). (B) Binary F-actin/S1 complex at a 1:1 molar ratio. (C) Comparison between F-actin (solid line)

from fitting the data in terms of discrete exponential components. In general, it requires at least three distinct lifetimes to adequately fit the data. Over 60% of the intensity has a short lifetime of 0.7 ms, 25% a lifetime of 6.0 ms, and only 12% a lifetime of 32.6 ms. The magnitude of the long lifetime component is in accord with the lifetime reported previously (Strambini and Lehrer, 1991), but its amplitude (12%) is less than was estimated previously (20%) from quantum yield data.

The phosphorescence decay was measured over the 0–30°C temperature range over which the average lifetime becomes increasingly shorter. At each temperature the analysis yields three lifetime components whose amplitude remains practically invariant throughout. By assuming that the shortening of τ_1 reflects an increased local mobility of the protein matrix surrounding a particular Trp residue, the temperature dependence of τ_1 would yield, through the empirical relationship established between lifetime (τ) and solvent viscosity (η) with model compounds (Strambini and Gonnelli, 1995), the activation enthalpy of the underlying structural fluctuations ($\ln 1/\eta = -\Delta H^\ddagger/RT + \text{const.}$). The values of ΔH^\ddagger are 13 ± 0.5 kcal/mol for τ_3 , 8.7 ± 0.6 kcal/mol for τ_2 , and 4.1 ± 1.4 kcal/mol for τ_1 . Only the activation enthalpy of τ_3 lies within the 10–30 kcal/mol range typical for compact internal regions of polypeptides, the only sites expected to be associated with long phosphorescence lifetimes. Smaller values are characteristic of flexible solvent-exposed sites but may also represent decays dominated by intramolecular quenching reactions.

Phosphorescence characteristics of actin complexed to the motor proteins MD/W– and S1

S1 contains eight Trp (Fig. 6) residues and their emission is likely to overlap and mask that of actin. Fig. 3 A shows that the spectrum of S1 is characterized by a single, relatively broad 0,0 vibrational band peaked at 409.1 nm, a wavelength intermediate between the red and blue bands of actin. Because of this fortunate circumstance, an analysis of the composite spectrum of the binary actin/S1 complex (in the region of the 0,0 vibrational band) in terms of S1 and actin components permits detecting eventual spectral changes induced by complex formation. The low temperature phosphorescence spectrum of the actin/S1 complex at a molar ratio of 1 is shown in Fig. 3 B. The spectrum of the complex is not simply a superposition of the separate components spectra. In particular, in the spectral region of the 0,0 vibrational band, the two peaks centered at 413.3 and 417.5 nm are peculiar of the complex as they are missing in the separate proteins. On the contrary, two shoulders, one at 405.0 nm and another at 409.3 nm, occur at the same

and the binary F-actin/MD/W– complex (dashed line) at a 1:1 molar ratio. $\lambda_{\text{ex}} = 295$ nm. The actin concentration is $10 \mu\text{M}$.

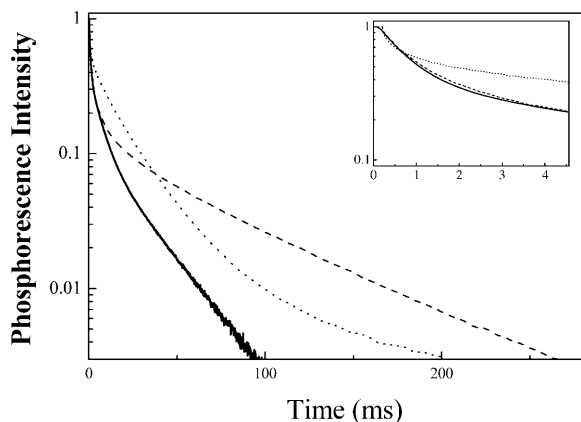


FIGURE 4 Trp phosphorescence decays of F-actin (solid line), S1 (dotted line), and of their binary complex (dashed line), at an actin/S1 molar ratio of 1:0.7, in aqueous phase at 273.5 K. (Inset) The decay during the first 10 ms. $\lambda_{\text{ex}} = 292$ nm. The curves are averages of 5–10 sweeps. The actin concentration is 10 μM .

wavelength of the blue band of actin and the single band of S1, respectively (Table 2).

The availability of a Trp-free motor domain (MD/W–) permits assigning the spectral changes of the complex to the individual protein components. The spectrum of actin is compared to that of the actin/MD/W– complex in Fig. 3 C. We note that the position of blue band of actin is unchanged in the complex, whereas the original components at 414.1 and 416.7 nm of the red band are replaced by a unique narrow band centered at 417.4 nm, practically the same wavelength of the 417.5-nm peak in the actin/S1 complex. The alteration of the red band of actin by MD/W– or S1 demonstrates that the binding of the motor protein modifies the environment of some of its internal residues, an indication that the process affects the internal structure of subdomain I. Further, the lack of the peak at 413.3 nm in the spectrum of the actin/MD/W– complex points out that this band must be attributed a red-shifted (from 409.1 to 413.3 nm) component of S1, implying that the structure of the motor protein is also affected on binding to actin.

The phosphorescence lifetime of S1 in buffer at ambient temperature is not considerably different from that of actin. The phosphorescence decay is heterogeneous and is again represented by at least three lifetime components in the same

submillisecond–millisecond range of actin (Fig. 4; Table 1). The phosphorescence of the actin/S1 complex, however, is characterized by a new long-lived component ($\tau_4 = 73$ ms) not present in the separate proteins (Table 1), implying that in either or both proteins the conformation about some Trp residue has changed, becoming distinctly more compact. At an actin/S1 molar ratio of 1:0.7 τ_4 is 9% and decreases to 5% when the ratio is lowered to 1:0.4. A decrease in amplitude at partial saturation roughly proportional to the amount of bound S1 suggests that τ_4 should be assigned to Trp residues in S1.

As with actin/MD/W– complex spectral changes, the ambiguity in the assignment of τ_4 is resolved. The results obtained at 100% saturation of the filament (actin/MD/W– molar ratio of 1:1.2) demonstrate that the long-lived emission (τ_4) does not belong to actin (Fig. 5) and consequently belongs to S1. The actin/MD/W– complex reveals subtle variations in all three lifetime components of actin that are masked in the S1 complex. As Table 1 and Fig. 5 indicate, the two short-lived components (τ_1 and τ_2) of actin decrease from 0.7 to 0.4 ms and from 6.0 to 3.8 ms, respectively, which means about a twofold change of the lifetime values. The long lifetime (τ_3) increases by 20%, from 32.6 to 39.0 ms. The amplitudes remain largely invariant. Although the decrease of τ_1 and τ_2 is consistent with a looser structure or more efficient quenching of the shorter-lived, presumably superficial Trp residues of actin, the increase of τ_3 indicates a tightening of the subunit core. The increased lifetime of some Trp residues in S1 indicates, in accord with spectral alterations, that a structural rearrangement occurs also in the motor protein making some region more compact and rigid.

Effect of tropomyosin on the phosphorescence characteristics of actin and of its complex with MD/W– and S1

The lack of Trp residues in Tm allows a direct comparison of the phosphorescence characteristics of actin filaments free and complexed to Tm. Binary and ternary complexes with MD/W– were formed in the presence of twofold excess Tm, relative to the 1:7 Tm/actin binding stoichiometry. Control runs with Tm alone confirmed no phosphorescence emission in buffer and only Tyr phosphorescence in low temperature glasses.

TABLE 1 Lifetime (amplitude) components derived from fitting the phosphorescence decay of actin samples in aqueous phase, at 0.5°C

Sample	τ_1 (ms)	(α_1)	τ_2 (ms)	(α_2)	τ_3 (ms)	(α_3)	τ_4 (ms)	(α_4)
F-actin	0.70	(62%)	6.0	(25%)	32.6	(13%)	–	–
F-actin/Tm	0.72	(63%)	5.9	(24%)	33.0	(13%)	–	–
F-actin/S1 (1:0.7)	0.56	(46%)	2.0	(33%)	13.6	(12%)	72.8	(9%)
F-actin/MD/W– (1:1.2)	0.40	(61%)	3.8	(26%)	39.0	(13%)	–	–
F-actin/MD/W–/Tm	0.38	(63%)	4.0	(25%)	40.0	(12%)	–	–

TABLE 2 Spectral peaks (λ_{00} at 140 K) and lifetime components (273.5 K) assigned to the tryptophans of actin

Sample	W79		W86		W340		W356	
	Spectral peak (nm)	Lifetime (ms)	Spectral peak (nm)	Lifetime (ms)	Spectral peak (nm)	Lifetime (ms)	Spectral peak (nm)	Lifetime (ms)
F-actin	404.5	0.7	?	0.7	416.7	32.6	414.1	6.0
F-actin + MD/W-	405.0	0.4	?	0.4	417.5	39.0	417.5	3.8
Structural environment	Solvent exposed		Buried but quenched by Cys ¹⁰		Buried and rigid		Shielded and flexible	

The emission of W89 is supposed to be largely quenched by proximal Cys¹⁰.

The binding of Tm to actin filaments has practically no influence on the phosphorescence characteristics of the actin component (Table 1). Indeed, the low temperature spectrum, the thermal quenching profile, the phosphorescence decay in buffer, and the temperature dependence of the three lifetime components, in the 0–30°C range, are remarkably similar to those of F-actin samples. Thus, according to the phosphorescence of its four Trp residues, the binding of Tm to the filament has practically no effect on both the structure and flexibility of subdomain I. Likewise, there are no visible effects of Tm binding to the binary actin/MD/W- and actin/S1 complexes in that the spectral and lifetime alterations of actin induced by its association to MD/W- or S1 are preserved also in the ternary complex.

DISCUSSION

Tentative assignment of the heterogeneous phosphorescence of actin to individual Trp residues

In proteins with few Trp residues, a heterogeneous multi-component phosphorescence emission can often be assigned to specific chromophores by matching various spectral/lifetime components to predictions made for each residue on the basis of their microenvironment (polarity, B-factors, and

proximity to quenching side chains) in the globular fold. Actin has four Trp residues, and according to the x-ray structure (Kabsch et al., 1990; Holmes et al., 1990) (Fig. 1) all are located in subdomain I. W79 and W356 are superficial, the former largely exposed to the solvent. W86 and W340 are more deeply buried. Being exposed to the aqueous phase, W79 should exhibit spectral and lifetime features similar to the chromophore free in solution ($\lambda_{0,0} \sim 406$ nm; $\tau \sim 0.5$ ms). W356 is shielded from the solvent, but its relatively large B-factors indicate that the residue is in a flexible segment of the polypeptide, sites characterized by relatively short lifetimes ($\tau \sim 1$ –10 ms). W86 and W340 are internal and have small B-factors, features normally conducive to long-lived phosphorescence ($\tau > 20$ ms). However, W86 is bound to be extensively quenched by Cys¹⁰ (Gonnelli and Strambini, 1995; Lapidus et al., 2001), which is only 4 Å from it. Based on the distance dependence of the quenching rate ($k(r) = 4.2 \times 10^9 \exp(-4r) \text{ s}^{-1}$; $r = \text{Å}$) (Lapidus et al., 2001), the lifetime of W86 is predicted to be less than 2 ms.

The high-resolution phosphorescence spectrum distinguishes three classes of chromophores (one contributes to the blue band and two to the red band of the spectrum), whereas the phosphorescence decay in buffer is characterized by at least three different lifetime components ($\tau_1 = 0.7$ ms, $\tau_2 = 6$ ms, and $\tau_3 = 33$ ms). If we assume a uniform conformation for F-actin, then each spectral/lifetime component refers to specific Trp residues. The spectral energy of the blue band, its thermal quenching profile, and a submillisecond lifetime are characteristic of solvent exposed Trps. There is little ambiguity in assigning this component to external W79. The contributors to the red band are necessarily internal chromophores. Among them, W340 is the only candidate for the long 33-ms lifetime, because W86 is quenched, and W356 exhibits large B-factors, indicative of a rather flexible site. The thermal profile links the long-lived emission to the peak at 416.7 nm (Fig. 3 A). The remaining peak at 414.1 nm is linked to the 6-ms lifetime component, and, because both features are consistent with the environment of W356, this emission should be assigned to it. Of course, one cannot exclude that a fourth spectral/lifetime component could be masked under any of the other three or that the energy transfer between W79 and W86, which are in close proximity, reduce the number of effective emitters to three. In conclusion, the above assignment of spectra and lifetimes

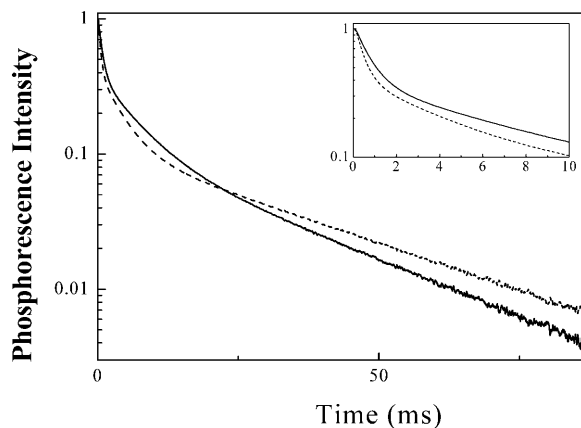


FIGURE 5 Comparison between the phosphorescence decay of F-actin (solid line) and its binary complex with MD/W- (dashed line) in aqueous phase at 273.5 K. The actin/MD/W- molar ratio is 1:1.2. $\lambda_{ex} = 292$ nm. The curves are averages of 5–10 sweeps. The actin concentration is 10 μM .

is straightforward for W79 (404.5 nm, τ_1) and W340 (416.7 nm, τ_3), it is quite reasonable for W356 (414.1 nm, τ_2), but less explicit for W86 (λ_{00} ?, τ_1).

The fluorescence spectrum is also an important indicator of the Trp environment. We note that fluorescence data obtained for single and triple Trp mutants of actin by Doyle et al. (2001) are in good accord with the nature of the Trp environment inferred from the phosphorescence properties assigned to the individual residues. W79 exhibits the most red-shifted fluorescence spectrum ($F_{max} = 335$ nm) indicative of a mobile polar site, typical of superficial residues partly exposed to the solvent. For W340 and W356, F_{max} is 328 nm, consistent with internal residues fully shielded from the solvent. Finally, the fluorescence emission of W86, which is buried, is weak, consistent with effective intramolecular quenching by nearby Cys¹⁰.

Changes of actin conformation induced by MD/W–, S1, and Tm

To learn about changes in the phosphorescence properties of actin, and indirectly of S1, that may be elicited by binding to the motor protein, we resorted to the Trp-free mutant motor domain from the *D. discoideum*, which is known to preserve the ATPase activity (Malnasi-Csizmadia et al., 2000). By assuming that the complex formed by MD/W– is analogous to that formed by S1, we may deduce changes in the structure and dynamics specific of the individual components. Trp phosphorescence demonstrated that binding of MD/W– affects the conformation of actin in various parts of subdomain I. This is inferred from the red shifts of the 414.1- and 416.7-nm spectral components to 417.5 nm (Fig. 3 C), an almost twofold reduction of τ_1 and τ_2 and about a 20% increase of τ_3 (Table 1). According to the assignment proposed above, the environment of W356 (414.1-nm peak and τ_2) of actin is the most affected by the interaction with the motor domain. W356 is wedged between two myosin docking patches on actin (Fig. 2). One patch is formed by Asp¹–Glu⁴, which binds S1 through an ionic interaction; the other is formed by hydrophobic Ile³⁴⁵ and Leu³⁴⁹, which are exposed to the surface of actin and make a stereospecific interaction with myosin. Although the red shift suggests a strengthening of the dipolar interaction with the triplet of W356, the reduction in lifetime is consistent with an increased conformational flexibility of the site. The latter is reminiscent of an induced fit type response where an optimization of actin-myosin contacts would occur at the cost of a looser packing in the region of W356.

W340 is buried in close vicinity of Ile³⁴², which is a potential stereo specific binding site of a helix-loop-helix motif (from Pro⁵²⁹ to Lys⁵⁵³) in the motor domain. Upon complexation to the motor domain, its spectrum is moderately perturbed, whereas the phosphorescence lifetime increases from 32.6 to 39 ms. This response entails a dampening of local

structural fluctuations as might be expected on forming larger protein aggregates.

In comparison to buried sites, the association of macromolecules is expected to alter more profoundly the environment of superficial side chains that become entrapped at the interface. The observation that the spectrum of W79 (the blue band), whose energy is largely dominated by the aqueous environment, is unchanged in the actin-myosin complex provides direct evidence that W79 is not part of the S1 docking surface. This finding is in accord with x-ray data indicating that W79 is quite far from the myosin-actin interface (Fig. 2) (Rayment et al., 1993). The reduction of its lifetime, on the other hand, suggests that subtle changes in conformation on the surface of actin are transmitted even to regions removed from the S1 binding site.

The possibility of discriminating between the phosphorescence of actin from that of S1, by comparison with the MD/W– mutant complex, has led to the discovery that also the structure of the motor protein is affected by binding to actin. Given the large number of Trps in skeletal myosin S1, however, it is not possible to be specific about the region or the extent of the conformational change. Both spectrum and lifetime indicate that the Trp residue/s involved is/are internal and that the polypeptide around some of them, judging from the emerging of a long phosphorescence lifetime ($\tau_4 = 72.8$ ms), becomes considerably more rigid in the complex. One possible candidate is W595 of S1, which in the complex becomes surrounded by the actin docking amino acids (Fig. 6). The fluorescence of W510 in the relay loop (Fig. 6) was shown to be also sensitive to nucleotide binding to the distant cleft in S1 (Malnasi-Csizmadia et al., 2001).

An important and somewhat unexpected result of this study is the apparent inertness of Tm binding on the phosphorescence characteristics of actin free or complexed to S1. According to the three-state dynamic steric model of thin filament regulation (McKillop and Geeves, 1993), in the absence of Troponin the thin filament is unregulated, Tm assuming two distinct positions on the filament depending on the presence or absence of S1. In the absence of S1, Tm lies over subdomains III and IV (Lorenz et al., 1995). In this

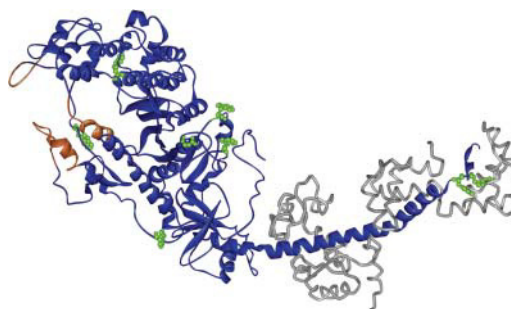


FIGURE 6 Solid ribbon model of skeletal myosin II S1 according to x-ray data from the Protein Data Bank, code 2MYS. The myosin heavy chain is blue, the light chains are gray, the Trps are green, and the actin binding regions are orange.

closed state, subdomain I is exposed, and Tm does not fully cover the myosin binding sites. In the presence of S1, Tm slides away from subdomain I and lies over subdomain IV. The filament is in the open state, and the myosin binding sites are fully exposed to allow the tight binding of S1 (McKillop and Geeves, 1993). The phosphorescence results are fully consistent with the above model of thin filament regulation as they confirm that in neither states the structure of subdomain I is affected by the association of Tm to actin (Table 1).

In summary, the reexamination of the phosphorescence properties of actin at higher resolution has led to an almost complete identification (with the exception of W86, suspected to be quenched) of the individual emission of its Trp residues, each of which will then represent a natural and independent probe of actin structure in specific sites of subdomain I. The results obtained with binary and ternary complexes with MD/W– or S1 and Tm emphasize that only the interaction with both of MD/W– and S1 affects the conformation of this actin domain. This finding and the inertness of Tm are nicely correlated to existing experimental evidence and prevailing models of actin-myosin interactions. These intrinsic probes will now be applied to enquire on the nature of the interactions between actin and myosin that characterize the closed and blocked functional states of the thin filament obtained in the presence of the troponin complex and modulated by Ca^{2+} .

The authors gratefully thank Krisztina Szarka and Dr. Mihály Kovács for excellent technical help in the preparation of the protein samples and the insightful comments from Dr. Miklós Nyitrai during the course of this work.

This work was supported by grants from the National Research Foundation (OTKA grants T32700 and T34442) and by the Research Group for Fluorescence Spectroscopy, Office for Academy Research Groups Attached to Universities and Other Institutions.

REFERENCES

- Berger, C. L., and D. D. Thomas. 1993. Rotational dynamics of actin-bound myosin heads in active myofibrils. *Biochemistry*. 32:3812–3821.
- Cioni, P., and G. B. Strambini. 1989. Dynamical structure of glutamate dehydrogenase as monitored by tryptophan phosphorescence. Signal transmission following binding of allosteric effectors. *J. Mol. Biol.* 207:237–247.
- Doyle, T., J. Hansen, and E. Reisler. 2001. Tryptophan fluorescence of yeast actin resolved via conserved mutations. *Biophys. J.* 80:427–434.
- Fiske, C. H., and Y. Subbarow. 1925. Determination of inorganic phosphate. *J. Biol. Chem.* 66:375–400.
- Gabellieri, E., S. Rahuel-Clermont, G. Branlant, and G. B. Strambini. 1996. Effects of NAD^+ binding on the luminescence of tryptophans 84 and 310 of glyceraldehyde-3-phosphate dehydrogenase from *Bacillus stearothermophilus*. *Biochemistry*. 35:12549–12559.
- Gonnelli, M., and G. B. Strambini. 1995. Phosphorescence lifetime of tryptophan in proteins. *Biochemistry*. 34:13847–13857.
- Hershberger, M. V., A. H. Maki, and W. C. Galley. 1980. Phosphorescence and optically detected magnetic resonance studies of a class of anomalous tryptophan residues in globular proteins. *Biochemistry*. 19:2204–2209.
- Holmes, K. C., D. Popp, W. Gebhard, and W. Kabsch. 1990. Atomic model of the actin filament. *Nature*. 347:44–49.
- Houk Jr., T. W., and K. Ue. 1974. The measurement of actin concentration in solution: a comparison of methods. *Anal. Biochem.* 62:66–74.
- Kabsch, W., H. G. Mannherz, D. Suck, E. F. Pai, and K. C. Holmes. 1990. Atomic structure of the actin:DNase I complex. *Nature*. 347:37–44.
- Lakos, Z., B. Somogyi, M. Balazs, J. Matko, and S. Damjanovich. 1990. The effect of transmembrane potential on the dynamic behavior of cell membranes. *Biochim. Biophys. Acta.* 1023:41–46.
- Lapidus, L., W. Eaton, and J. Hofrichter. 2001. Dynamics of intramolecular contact formation in polypeptides: distance dependence of quenching rates in a room-temperature glass. *Phys. Rev. Lett.* 87:258101.
- Lorenz, M., K. J. Poole, D. Popp, G. Rosenbaum, and K. C. Holmes. 1995. An atomic model of the unregulated thin filament obtained by X-ray fiber diffraction on oriented actin-tropomyosin gels. *J. Mol. Biol.* 246:108–119.
- Lorinczy, D., N. Hartvig, and J. Belagyi. 2002. Analysis of nucleotide myosin complexes in skeletal muscle fibres by DSC and EPR. *J. Biochem. Biophys. Methods.* 53:75–87.
- Malnasi-Csizmadia, A., M. Kovacs, R. J. Woolley, S. W. Botchway, and C. R. Bagshaw. 2001. The dynamics of the relay loop tryptophan residue in the Dictyostelium myosin motor domain and the origin of spectroscopic signals. *J. Biol. Chem.* 276:19483–19490.
- Malnasi-Csizmadia, A., R. J. Woolley, and C. R. Bagshaw. 2000. Resolution of conformational states of Dictyostelium myosin II motor domain using tryptophan (W501) mutants: implications for the open-closed transition identified by crystallography. *Biochemistry*. 39:16135–16146.
- Margossian, S. S., and S. Lowey. 1982. Preparation of myosin and its subfragments from rabbit skeletal muscle. *Methods Enzymol.* 85:55–71.
- McKillop, D. F., and M. A. Geeves. 1993. Regulation of the interaction between actin and myosin subfragment 1: evidence for three states of the thin filament. *Biophys. J.* 65:693–701.
- Norby, J. G. 1971. Studies on a coupled enzyme assay for rate measurements of ATPase reactions. *Acta Chem. Scand.* 25:2717–2726.
- Nyitrai, M., G. Hild, J. Belagyi, and B. Somogyi. 1999. The flexibility of actin filaments as revealed by fluorescence resonance energy transfer. The influence of divalent cations. *J. Biol. Chem.* 274:12996–13001.
- Nyitrai, M., G. Hild, Z. Lakos, and B. Somogyi. 1998. Effect of Ca^{2+} - Mg^{2+} exchange on the flexibility and/or conformation of the small domain in monomeric actin. *Biophys. J.* 74:2474–2481.
- Ostap, E. M., and D. D. Thomas. 1991. Rotational dynamics of spin-labeled F-actin during activation of myosin S1 ATPase using caged ATP. *Biophys. J.* 59:1235–1241.
- Rayton, I., H. M. Holden, M. Whittaker, C. B. Yohn, M. Lorenz, K. C. Holmes, and R. A. Milligan. 1993. Structure of the actin-myosin complex and its implications for muscle contraction. *Science*. 261:58–65.
- Schauerer, J. A., D. G. Steel, and A. Gafni. 1997. Time-resolved room temperature tryptophan phosphorescence in proteins. *Methods Enzymol.* 278:49–71.
- Silva, N. D. J., and F. G. Prendergast. 1996. Tryptophan dynamics of the FK506 binding protein: time-resolved fluorescence and simulatins. *Biophys. J.* 70:1122–1137.
- Smillie, L. B. 1982. Preparation and identification of alpha- and beta-tropomyosins. *Methods Enzymol.* 85:234–241.
- Somogyi, B., and Z. Lakos. 1993. Protein dynamics and fluorescence quenching. *J. Photochem. Photobiol. B.* 18:3–16.
- Somogyi, B., Z. Lakos, A. Szarka, and M. Nyitrai. 2000. Protein flexibility as revealed by fluorescence resonance energy transfer: an extension of the method for systems with multiple labels. *J. Photochem. Photobiol. B.* 59:26–32.
- Spudich, J. A., and S. Watt. 1971. The regulation of rabbit skeletal muscle contraction. I. Biochemical studies of the interaction of the tropomyosin-troponin complex with actin and the proteolytic fragments of myosin. *J. Biol. Chem.* 246:4866–4871.

- Strambini, G. B., and M. Gonnelli. 1990. Tryptophan luminescence from liver alcohol dehydrogenase in its complexes with coenzyme. A comparative study of protein conformation in solution. *Biochemistry*. 29: 196–203.
- Strambini, G. B., and M. Gonnelli. 1995. Tryptophan phosphorescence in fluid solution. *J. Am. Chem. Soc.* 117:7646–7651.
- Strambini, G. B., and S. S. Lehrer. 1991. Tryptophan phosphorescence of G-actin and F-actin. *Eur. J. Biochem.* 195:645–651.
- Vanderkooi, J. M. 1992. Tryptophan phosphorescence from proteins at room temperature. *In* Topics in Fluorescence Spectroscopy, Vol. 3. J. R. Lakowicz, editor. Plenum Press, New York. 113–136.
- Wagner, P. D. 1977. Fractionation of heavy meromyosin by affinity chromatography. *FEBS Lett.* 81:81–85.
- Wakelin, S., P. B. Conibear, R. J. Woolley, D. N. Floyd, C. R. Bagshaw, M. Kovacs, and A. Malnasi-Csizmadia. 2002. Engineering *Dictyostelium discoideum* myosin II for the introduction of site-specific fluorescence probes. *J. Muscle Res. Cell Motil.* 23:673–83.
- Weeds, A. G., and R. S. Taylor. 1975. Separation of subfragment-1 isoenzymes from rabbit skeletal muscle myosin. *Nature.* 257:54–56.
- Zavodszky, P., J. Kardos, Svingor, and G. A. Petsko. 1998. Adjustment of conformational flexibility is a key event in the thermal adaptation of proteins. *Proc. Natl. Acad. Sci. USA.* 95:7406–7411.